Journal of Catalysis 287 (2012) 86–92

Contents lists available at SciVerse ScienceDirect

Journal of Catalysis

journal homepage: www.elsevier.com/locate/jcat

Effect of the nature of rhodium catalyst supports on initiation of H_2 production during *n*-butane oxidative reforming at room temperature

Katsutoshi Nagaoka [a,*], Katsutoshi Sato [a,b], Yusaku Takita [a]

[a] Department of Applied Chemistry, Faculty of Engineering, Oita University, 700 Dannoharu, Oita City, Oita 870-1192, Japan
[b] Fuel Cell System Group, Energy Technology Research Institute, National Institute of Advanced Industrial Science and Technology (AIST), Umezono 1-1-1, Tsukuba 305-8568, Japan

ARTICLE INFO

Article history:
Received 19 October 2011
Revised 26 November 2011
Accepted 2 December 2011
Available online 21 January 2012

Keywords:
Oxidative reforming
H_2 production
Room temperature
Rhodium
Rare earth oxide
Redox property
OSC

ABSTRACT

Three rhodium catalysts supported on rare earth oxides with redox properties, Rh/CeO_2, Rh/Pr_6O_{11}, and Rh/Tb_4O_7, were tested for their ability to trigger oxidative reforming of *n*-butane at room temperature. Only Rh/CeO_2 triggered the oxidative reforming, owing to the heat generated by the spontaneous oxidation of the CeO_{2-x} species produced by prior reduction of the supported catalyst with H_2. Although the three rare earth oxides were reduced to $CeO_{1.91}$, Pr_2O_3, and Tb_2O_3, respectively, by H_2 at $\geqslant$873 K, $CeO_{1.91}$ was the only reduced oxide that was oxidized upon exposure to O_2 at room temperature. These results indicate that the ability of the reduced oxide support to undergo oxidation at room temperature was crucial for triggering oxidative reforming of *n*-butane at room temperature.

1. Introduction

Hydrogen has the potential to provide electricity much more efficiently than combustion processes, particularly when it is used for fuel cells, which convert chemical energy directly into electrical energy and thus are not limited by Carnot efficiencies. Therefore, H_2 fuel cells are expected to partially solve problems arising from the limited supply of fossil fuels [1,2]. However, innovations in fuel-cell catalyst materials, fuel-cell engineering, and the reforming of hydrocarbons to produce H_2 are needed if this technology is to compete with conventional electrical power plants [3,4]. In this context, the oxidative reforming (OR) of liquid fuels such as liquefied petroleum gas, gasoline, diesel fuel, and alcohol (all of which can be easily stored and transported) to produce H_2-rich reformate gas is of great interest [5–12]. Because OR is a combination of exothermic (combustion) and endothermic (reforming) reactions [13–16], it is expected to be more suitable than conventional steam reforming for the local production of H_2 at filling stations and at on-site reformers for domestic fuel cells, for which start-up and shutdown processes are frequently repeated [17].

Efficient start-up of a reformer requires a short start-up time, overall energy efficiency, and catalyst stability [3]. The most crucial criterion, however, is the catalytic autoignition temperature that normally exceeds 473 K even in the presence of noble metal catalysts [8]. To achieve such temperatures, researchers have explored several strategies, including electrical heating of catalysts [18] and homogeneous combustion [19,20]. Electrical heating is more practical because it is safer and does not require a complex start-up procedure. However, this strategy requires external energy for heating the catalysts from room temperature to at least 473 K, as well as adequate time for heating; and the resulting time lapse delays the onset of H_2 production.

In previous work, we demonstrated a new Rh/CeO_2-catalyzed cold-start OR process triggered rapidly at room temperature without the need for external energy input or a specialized start-up procedure (Fig. 1) [17]. This process can be expected to permit the development of self-sufficient reforming systems for a new generation of fuel-cell applications. Prior to the reforming reaction, the Rh/CeO_2 catalyst is reduced in a H_2 atmosphere at $\geqslant$873 K, and then OR of *n*-butane (*n*-C_4H_{10}), the main component of liquid petroleum gas, is triggered in the presence of the catalyst at room temperature ($\sim$300 K). The heat produced by re-oxidation of CeO_{2-x} to CeO_2 rapidly increases the catalyst temperature from room temperature to the catalytic autoignition temperature (520 K) and drives the overall reaction such that 90% of the *n*-C_4H_{10} is reformed. In subsequent cycles, OR is repeatedly triggered at room temperature by *in situ* reduction of CeO_2 by H_2 produced during OR, provided that the catalyst is cooled without exposure to air.

In this new catalytic OR process, CeO_2 provides oxygen storage capacity (OSC), that is, it alternately takes up and releases oxygen. OSC is useful in several other catalytic processes including catalytic

* Corresponding author. Fax: +81 97 554 7979.
E-mail address: nagaoka@cc.oita-u.ac.jp (K. Nagaoka).

0021-9517/$ - see front matter © 2011 Elsevier Inc. All rights reserved.
doi:10.1016/j.jcat.2011.12.007

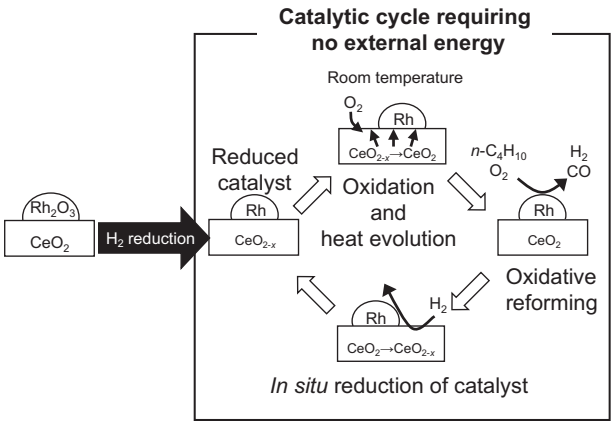

Fig. 1. Schematic of the catalytic system developed for n-C_4H_{10} oxidative reforming.

oxidation [21–27] and the automotive three-way reaction [28–32]. Our catalytic OR process represents a new application of an oxygen storage material. In the current study, we investigated the potential of other rare earth oxides to act as oxygen storage materials in the OR process. The rare earth elements Ce, Pr, and Tb have trivalent and quadrivalent oxidation states, and oxides of these elements exist as cubic fluorite-type structures (CeO_2, Pr_6O_{11}, and Tb_4O_7) and as hexagonal A- or cubic bixbyite C-type rare earth sesquioxide structures (Ce_2O_3, Pr_2O_3, and Tb_2O_3) [33]. Thus, their single-component oxides and solid solutions show OSC [24,26,31,34–37]. We evaluated Pr_6O_{11} and Tb_4O_7 as well as CeO_2 as supports for the Rh catalyst in the new catalytic OR process, and we determined the physicochemical and redox properties that make a catalyst support suitable for the OR process. We also discuss the role of Rh in the OR process.

2. Experimental

2.1. Catalyst preparation

We used three rare earth oxide–supported Rh catalysts: Rh/CeO_2, Rh/Pr_6O_{11}, and Rh/Tb_4O_7. Rh supported on Al_2O_3, which is irreducible under the OR conditions, was used as a reference catalyst. CeO_2 (JRC-CEO3) and γ-Al_2O_3 (JRC-ALO3) were supplied by the Catalysis Society of Japan. Pr_6O_{11} and Tb_4O_7 supports were precipitated at room temperature from suspensions prepared by adding a solution of $Pr(NO_3)_3$ $6H_2O$ or $Tb(NO_3)_3$ $6H_2O$ to 25% NH_3 solution. The precipitates were kept in suspension by stirring at room temperature overnight and were then filtered, washed with distilled water, and dried overnight at 353 K. All the rare earth oxide supports were calcined at 1073 K and wet impregnated with an aqueous solution of $Rh(NO_3)_3{\cdot}nH_2O$. The final concentration of Rh was 1 wt.%. The impregnated samples were dried at room temperature and subsequently at 373 K overnight and then calcined at 723 K in flowing air. The obtained catalyst powders were pressed into pellets at 52 MPa for 5 min. The pellets were crushed and sieved to obtain grains with diameters between 180 and 250 μm. These resulting grains were characterized and used in the activity tests.

2.2. Activity tests

Catalyst (200 mg) was loaded into a tubular quartz reactor (i.d. = 7 mm). Quartz wool was packed around the catalyst inside the reactor, and then α-Al_2O_3 pellets (d = 1 mm) were packed into the remaining space to reduce heat loss during the catalytic tests under quasi-adiabatic conditions. A K-type thermocouple (d = 0.5 mm) was inserted into the catalyst bed through the α-Al_2O_3 and quartz wool packing. Cylinders of research-grade gas were used for all experiments. The catalysts were heated in a pure H_2 atmosphere at a rate of 10 K min^{-1} and kept at 473, 673, 873, or 1073 K for 1 h, and then the reactor was purged with pure Ar for 1 h at 873 K and subsequently cooled to room temperature (~300 K). The furnace was switched off and opened, and the quartz reactor was wrapped with ceramic insulation for subsequent reaction under quasi-adiabatic conditions. The setup for the activity test has been described in detail elsewhere [17]. The furnace heater remained switched off from this point on. An n-$C_4H_{10}/O_2/Ar/N_2$ feed gas mixture (molar ratio = 1:2:7:1; space velocity = 122 L h^{-1} g^{-1}) was passed over the catalyst at room temperature. We determined the feed gas composition by assuming the following stoichiometric OR reaction:

$$n\text{-}C_4H_{10} + 2O_2 \rightarrow 4CO + 5H_2 \quad \Delta H_{298K} = -316\ \text{kJ} \tag{1}$$

The composition of the exit gases was continuously monitored with a quadrupole mass spectrometer (ANELVA, M-201QA-TDM). After 30 min, the reaction products were also analyzed by means of a gas chromatograph equipped with a thermal conductivity detector (TCD; Agilent, 6890 N). After 35 min, we terminated the reaction by replacing the feed gas with Ar and cooling the catalyst to room temperature. This feed–purge sequence was repeated five more times.

2.3. Characterization of the catalysts

The specific surface area of the catalysts after calcination was determined by the Brunauer–Emmett–Teller method.

We measured CO chemisorption by catalyst samples using the O_2–CO_2–H_2–CO pulse procedure proposed by Takeguchi et al. [38]. O_2 was fed to each sample at 30 mL min^{-1} during programed heating to 573 K. The sample was maintained at the temperature for 30 min, cooled to room temperature, and flushed with He for 5 min. Following the oxidation, the sample was treated with H_2 at 473 K for 1 h and then cooled to 323 K. At the temperature, it was flushed with He for 30 min and exposed to O_2 for 5 min, to CO_2 for 5 min, to He for 5 min, and to H_2 for 5 min and then the sample was purged with He gas for 30 min. Finally, CO chemisorption was carried out at 323 K in a He stream (30 mL min^{-1}) by means of a pulsed-chemisorption technique with CO at 8.9 μmol per pulse. CO/Rh = 1 was assumed to calculate Rh dispersion.

Temperature-programed reduction (TPR) measurements were taken over 200 mg of each catalyst from room temperature to 1273 K (10 K min^{-1}) in flowing H_2/Ar gas (H_2/Ar = 1/19, 30 mL min^{-1}). The H_2 consumption was monitored with a TCD.

The uptake of O_2 at 323 K on the reduced catalysts was measured by means of pulse injection. Each catalyst was loaded into a tubular U-shaped quartz reactor and reduced in pure H_2 at 473, 673, 873, or 1073 K, and then the reactor was flushed with Ar at 873 K. Pulses of pure O_2 (95.5 μmol per pulse) were injected into the catalyst bed at 323 K, and the O_2 uptake was measured with a TCD. The pulses were continued until the level of O_2 absorption stabilized, indicating that the maximum amount of O_2 had been absorbed.

X-ray diffraction (XRD) analysis was performed with a Rigaku RINT-2000 X-ray diffractometer with monochromatized Cu-K_α radiation. The samples were transferred to the sample stage of the XRD instrument after reductive treatment at the various temperatures.

Thermogravimetric (TG) measurements were taken from room temperature to 1073 K under flowing air with a Rigaku Thermo plus TG8120. For the TG measurements, we used the samples that had been used for XRD analysis after reduction at 873 K.

3. Results and discussion

3.1. Activity tests for triggering OR at room temperature

We determined the dry gas product concentrations immediately after supplying the feed gas at room temperature to Rh/CeO_2 reduced at 873 K (Fig. 2). At the beginning of the process (4 s), CO and CO_2 were the only products, but after that time, the H_2 concentration increased drastically and eventually greatly exceeded the CO and CO_2 concentrations. This H_2 concentration increase occurred simultaneously with the increase in the catalyst bed temperature, indicating that first combustion (Eq. (2)) and then reforming (Eqs. (3) and (4)) of n-C_4H_{10} were initiated sequentially:

$$n\text{-}C_4H_{10} + 6.5O_2 \rightarrow 4CO_2 + 5H_2O \quad \Delta H_{298K} = -2657\ \text{kJ} \tag{2}$$

$$n\text{-}C_4H_{10} + 4CO_2 \rightarrow 8CO + 5H_2 \quad \Delta H_{298K} = -816\ \text{kJ} \tag{3}$$

$$n\text{-}C_4H_{10} + 4H_2O \rightarrow 4CO + 9H_2 \quad \Delta H_{298K} = -651\ \text{kJ} \tag{4}$$

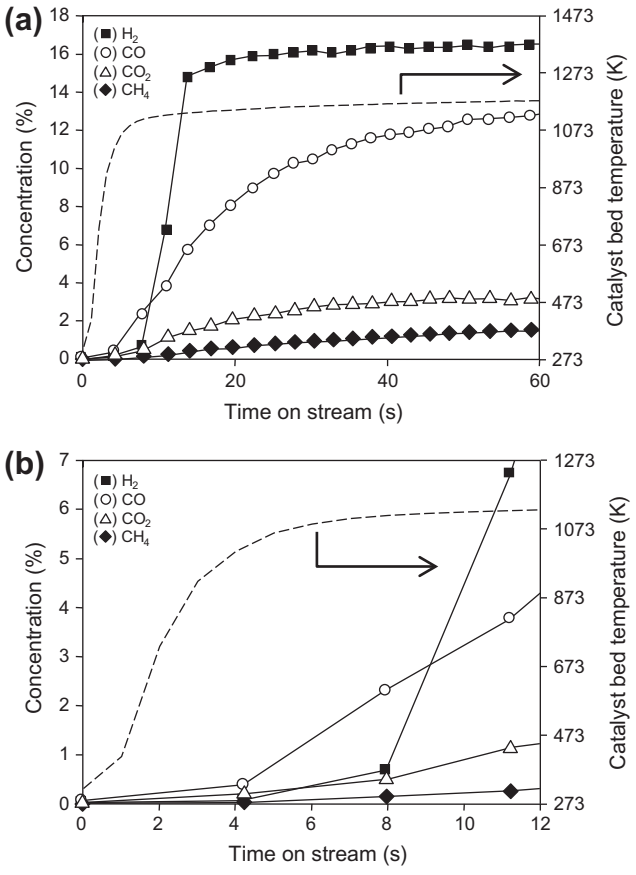

Fig. 2. Time dependence of product concentrations in dry gas and catalyst bed temperature during OR over Rh/CeO_2 reduced at 873 K: (a) 0–60 s and (b) 0–12 s.

Additionally, a part of O_2 must be consumed by oxidation of the Rh and CeO_{2-x} at that moment. This may explain higher CO concentration than CO_2 concentration at 4 s.

The formation of CH_4 at low concentrations indicates that the methanation of CO or CO_2 occurred (Eqs. (5) and (6))[39,40]:

$$CO + 3H_2 \rightarrow CH_4 + H_2O \quad \Delta H_{298K} = -206\ \text{kJ} \tag{5}$$

$$CO_2 + 4H_2 \rightarrow CH_4 + 2H_2O \quad \Delta H_{298K} = -165\ \text{kJ} \tag{6}$$

Note that the occurrence of methanation is discussed in Section 3.4, on the basis of results of activity tests. After 14 s, the H_2 concentration increased to 15%, which was 79% of the steady-state concentration, and the catalyst bed temperature was 1133 K. At that time, the heats of the exothermic and endothermic reactions, as well as the external heat losses, were balanced. Note that atomic hydrogen formed during reduction with H_2 and remained on the catalyst, which might have contributed to the triggering mechanism, was removed by Ar purge at 873 K after H_2 reduction. The results shown in the figure indicate that OR was triggered quickly over reduced Rh/CeO_2 without any external heat input.

OR was triggered at room temperature over Rh/CeO_2 that had been reduced at $\geqslant$873 K (Table 1). Even in the absence of external heat input, complete conversion of O_2 and 90% conversion of n-C_4H_{10} were achieved. The H_2 yield and formation rate were high ($\geqslant$79% and 44 L h^{-1} g^{-1}, respectively). In contrast, OR was not triggered over Rh/Pr_6O_{11}, Rh/Tb_4O_7, or Rh/Al_2O_3. The catalyst bed temperatures rose only slightly upon exposure to the reaction mixture, which indicates that only minor oxidation of the catalyst occurred. Neither oxidation nor reforming of n-C_4H_{10} was observed with these catalysts. Al_2O_3 is irreducible under the reduction conditions we used, and oxidation of metallic Rh alone was insufficient to heat the catalyst to the catalytic autoignition temperature. We concluded that for Rh/CeO_2 reduced at 873 and 1073 K, an additional reaction, namely oxidation of CeO_{2-x} to CeO_2, provided additional heat to bring the catalysts to the catalytic autoignition temperature (520 K) [17]. The reason that OR was not triggered at room temperature over Rh/Pr_6O_{11} and Rh/Tb_4O_7 reduced with H_2 was not clear. To find an explanation, we characterized the supported Rh catalysts as described in Section 3.2.

3.2. Characterization of the catalysts

3.2.1. Physicochemical properties of the catalysts

We determined various physicochemical properties of the supported Rh catalysts (Table 2). The specific surface areas of the three rare earth oxide–supported catalysts were smaller than the specific surface area of Rh/Al_2O_3; in particular, the specific surface areas of Rh/Pr_6O_{11} and Rh/Tb_4O_7 were lower than 10 m^2 g^{-1}. The specific surface area seemed to affect the Rh dispersion, which decreased with decreasing specific surface area. One may suspect that difference in catalytic property is ascribed to the difference in specific surface area of the catalysts. However, even if Rh was supported on CeO_2 of which specific surface area was 3 m^2 g^{-1} and on which Rh dispersion was 27.0%, OR was triggered at room temperature over the catalyst reduced at 873 K. These results indicate that cru-

Table 1
Catalytic activity of supported Rh catalysts reduced at different temperatures in OR, measured after 30 min.

Catalyst	Reduction temperature (K)	Conversion (%)		Yield of products (%)				H_2 formation rate (L h^{-1} g^{-1})
		n-C_4H_{10}	O_2	H_2	CO_2	CO	CH_4	
Rh/CeO_2	873	97	100	79	6	84	8	44
	1073	91	100	83	5	85	1	46

Neither n-C_4H_{10} nor O_2 was converted over Rh/Al_2O_3, Rh/Pr_6O_{11}, and Rh/Tb_4O_7 regardless of reduction temperature.

Table 2
Physicochemical properties of supported Rh catalysts.

Catalyst	Specific surface area[a] ($m^2\ g^{-1}$)	CO adsorption[b] ($\mu mol\ g^{-1}$)	Dispersion of Rh (%)
Rh/Al_2O_3	114	89	92
Rh/CeO_2	47	32	33
Rh/Pr_6O_{11}	8	13	13
Rh/Tb_4O_7	2	5	6

[a] After calcination.
[b] After reduction at 873 K.

cial properties of the catalysts for triggering OR are mainly dependent on the kind of the rare earth elements.

3.2.2. Redox properties of the catalysts

As already mentioned (see Fig. 1), the heat produced by oxidation of the catalyst support heated the catalyst to the catalytic autoignition temperature and initiated OR. Therefore, reduction and subsequent oxidation of the catalyst supports were key steps for triggering OR at room temperature. We evaluated the reduction of the supported catalysts by TPR (Fig. 3). In the TPR profile of Rh/Al_2O_3, a tiny broadened peak for H_2 uptake due to the reduction of Rh_2O_3 was visible at around 463 K. In contrast, larger H_2 uptake peaks compared to the reduction of Rh_2O_3 were observed for the other catalysts, which indicate the reduction of the rare earth oxides. In the case of Rh/CeO_2, H_2 uptake due to reduction of CeO_2 started above 773 K. For Rh/Pr_6O_{11} and Rh/Tb_4O_7, rapid H_2 uptake due to reduction of Rh_2O_3 and Pr_6O_{11} and Tb_4O_7 started at temperatures below 473 K. These results indicate that Rh/Pr_6O_{11} and Rh/Tb_4O_7 were reduced at lower temperatures than Rh/CeO_2, and thus the inability of Rh/Pr_6O_{11} and Rh/Tb_4O_7 to trigger OR could not be ascribed to insufficient reduction of the catalytic supports.

Next, we evaluated O_2 absorption by the reduced catalysts by pulsing O_2 into the catalyst bed at 323 K (Fig. 4). Because Al_2O_3 is irreducible under the reduction conditions employed, the O_2 absorption was nearly equal to the theoretical value for the oxidation of Rh to Rh_2O_3 (73 $\mu mol\ g^{-1}$). The uptake of O_2 on Rh/CeO_2 reduced at 673 K was similar to that observed for Rh/Al_2O_3, whereas the uptake of O_2 increased drastically for the catalysts reduced at the higher reduction temperatures. These results indicate that

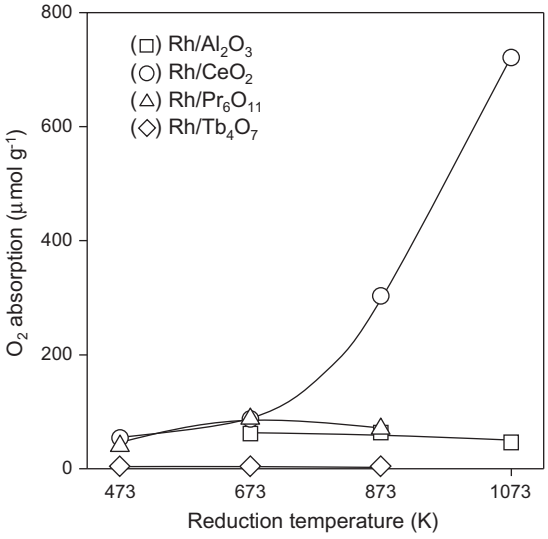

Fig. 4. O_2 absorption capacity at 323 K for supported Rh catalysts reduced at different temperatures.

CeO_2 was reduced to CeO_{2-x} at 873 and 1073 K, in agreement with the TPR results, and that the oxidation of CeO_{2-x} increased the uptake of O_2 at 323 K.

Although TPR showed that Rh/Pr_6O_{11} and Rh/Tb_4O_7 were easily reduced, the uptake of O_2 by these catalysts did not exceed 87 $\mu mol\ g^{-1}$ even after reduction at 873 K. These results indicate that Pr_2O_3 and Tb_2O_3 were not oxidized at 323 K.

3.2.3. Catalyst structures before and after H_2 reduction

To elucidate changes in the catalyst structure during H_2 reduction, we measured the XRD patterns of the supported Rh catalysts before and after reduction (shown for Rh/CeO_2 in Fig. 5). All the samples, fresh and reduced at 473 or 873 K, showed the diffraction pattern for the fluorite structure ($a = b = c = 0.541$ nm). Peak shift due to the change of lattice parameter was not observed. However, the peak intensity was higher at the higher reduction temperature, owing to sintering of the material.

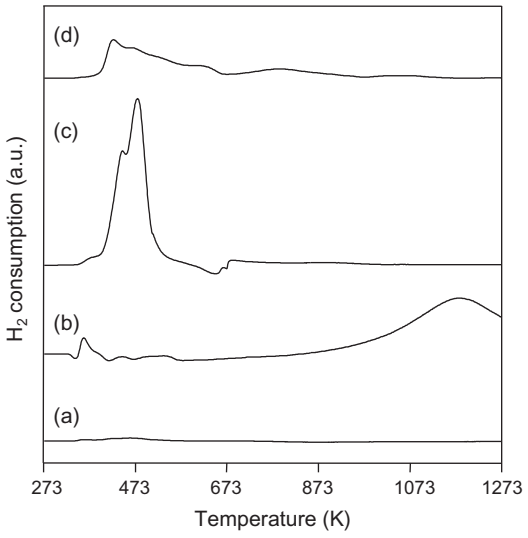

Fig. 3. Temperature-programed reduction profiles for (a) Rh/Al_2O_3, (b) Rh/CeO_2, (c) Rh/Pr_6O_{11}, and (d) Rh/Tb_4O_7.

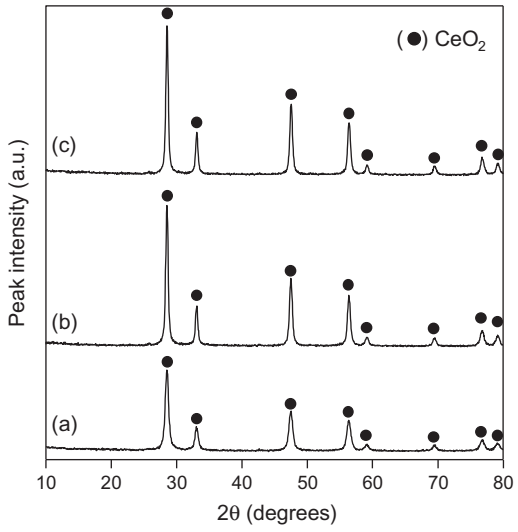

Fig. 5. XRD patterns of Rh/CeO_2 catalysts reduced at different temperatures: (a) fresh, (b) 473 K, and (c) 873 K.

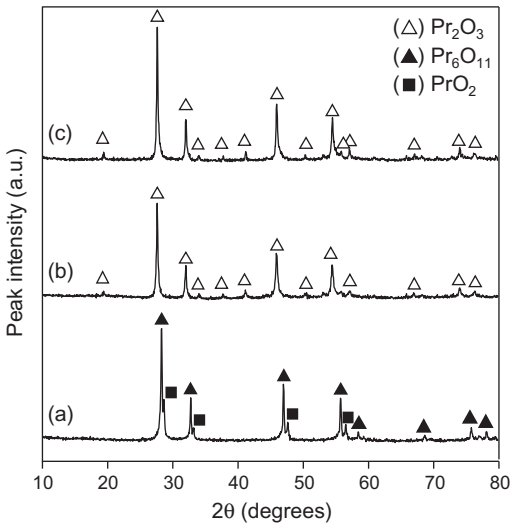

Fig. 6. XRD patterns of Rh/Pr_6O_{11} catalysts reduced at different temperatures: (a) fresh, (b) 473 K, and (c) 873 K.

In contrast, for Rh/Pr_6O_{11}, the fluorite structure corresponding to Pr_6O_{11} and PrO_2 observable for the fresh catalyst was not observed after reduction at 473 and 873 K. Instead, negative shifts, e.g., $2\theta = 1.0°$ for the peak of (220) of Pr_6O_{11} at 47.0°, which indicated lattice expansion and formation of new peaks due to the formation of Pr_2O_3 with a C-type rare earth sesquioxide structure were observed after reduction at 473 K and the intensity of the peaks for this phase increased after reduction at 873 K owing to sintering (Fig. 6). Lattice constants estimated by using the (220) peak of cubic fluorite and (440) peak of cubix bixbyite sesquioxide structures were 0.546 and 1.12 nm for Rh/Pr_6O_{11} and Rh/Pr_2O_3, respectively. These results indicate that Pr_6O_{11} and PrO_2 were already reduced to Pr_2O_3 at around 473 K and that the formed Pr_2O_3 was not re-oxidized upon exposure to the atmosphere at room temperature. Because Pr_2O_3 was not re-oxidized, the heat produced by the oxidation of the catalysts was insufficient to heat the catalyst to the autoignition temperature.

In the case of Rh/Tb_4O_7 (Fig. 7), which also did not absorb O_2 after reduction, the diffraction peaks of Tb_4O_7 visible in the fresh sample were shifted to smaller angles after reduction at 473 K; these shifted peaks were ascribed to Tb_2O_3 with a C-type rare earth sesquioxide structure. Owing to the phase transition from Tb_4O_7 to Tb_2O_3, the peak intensities seemed to be decreased. When the reduction temperature was increased to 873 K, the peak intensities increased, and other peaks for Tb_2O_3 were formed. Lattice constants estimated by using the (220) peak of cubic fluorite and (440) peak of cubix bixbyite sesquioxide structures were 0.528 and 1.07 nm for Rh/Tb_4O_7 and Rh/Tb_2O_3, respectively. Hence, like Pr_6O_{11}, Tb_4O_7 was reduced to Tb_2O_3 at 473 K but was not re-oxidized upon exposure to the atmosphere at room temperature. Therefore, there was insufficient heat to bring the catalyst to the catalytic autoignition temperature for OR.

3.2.4. Oxidation of reduced rare earth oxides in Rh catalysts

To ensure the heat evolution by the oxidation of CeO_{2-x} at room temperature, an O_2/Ar mixture was passed over Rh/CeO_2 that was reduced at 873 K. As shown in Fig. 8, the temperature of the catalyst bed increased to 513 K within 4 s. The rapid increase indicates that the oxidation of CeO_{2-x} provided sufficient heat in the catalyst bed to trigger the oxidation of n-C_4H_{10} and its subsequent reforming. In contrast, when Rh/Pr_6O_{11} and Rh/Tb_4O_7 were reduced at 873 K, such increases in catalyst bed temperatures were not observed. Therefore, it was revealed that Pr_2O_3 and Tb_2O_3 were stable and not oxidized upon exposure to the atmosphere at room temperature, which was in agreement with the results of O_2 absorption and XRD measurements.

To understand the oxidation behavior of the reduced rare earth oxides in the Rh catalysts, we conducted TG measurements of the catalyst samples used for XRD measurements. The samples were heated to 873 K under a H_2 flow, and the TG measurements were taken under an air flow (Fig. 9). Rh/CeO_2 did not show weight change during the measurement. In contrast, reduced Rh/Pr_6O_{11} and Rh/Tb_4O_{10} exhibited weight increases starting at approximately 373 and 573 K, respectively. These results clearly indicate that a temperature of at least 373 or 573 K was necessary for the oxidation of Pr_2O_3 and Tb_2O_3. In contrast, reduced Rh/CeO_2 was oxidized completely to CeO_2 on exposure to the atmosphere at room temperature. By assuming that complete oxidation to CeO_2 and Rh_2O_3 occurred during O_2 absorption measurements (Fig. 4), we determined that the CeO_{2-x} species after the reduction of Rh/CeO_2 at 873 and 1073 K had average stoichiometries of $CeO_{1.91}$ and $CeO_{1.77}$, respectively. Taking these results together with the re-

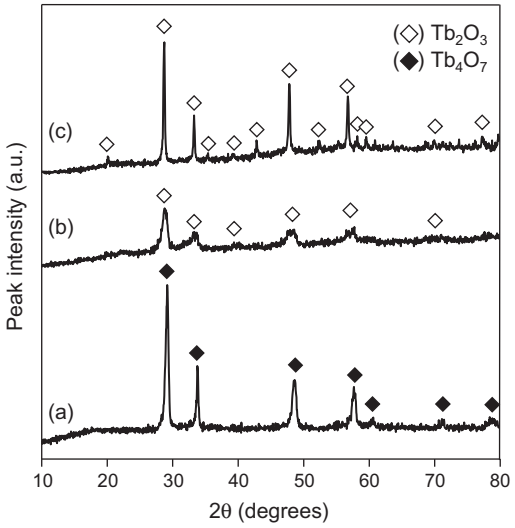

Fig. 7. XRD patterns of Rh/Tb_4O_7 catalysts reduced at different temperatures: (a) fresh, (b) 473 K, and (c) 873 K.

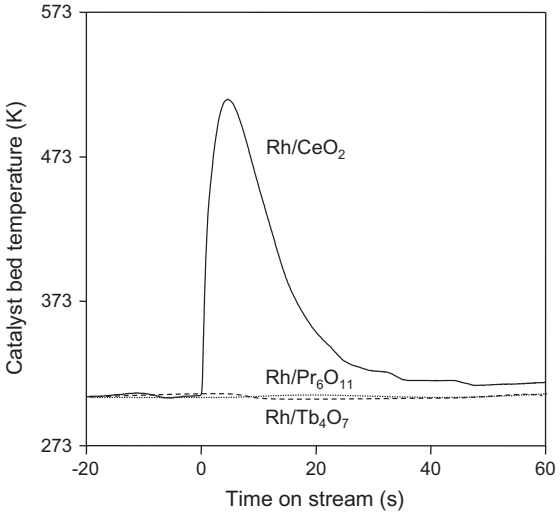

Fig. 8. Time dependence of catalyst bed temperatures with the exposure of O_2/Ar to Rh/CeO_2, Rh/Pr_6O_{11}, and Rh/Tb_4O_7 reduced at 873 K.

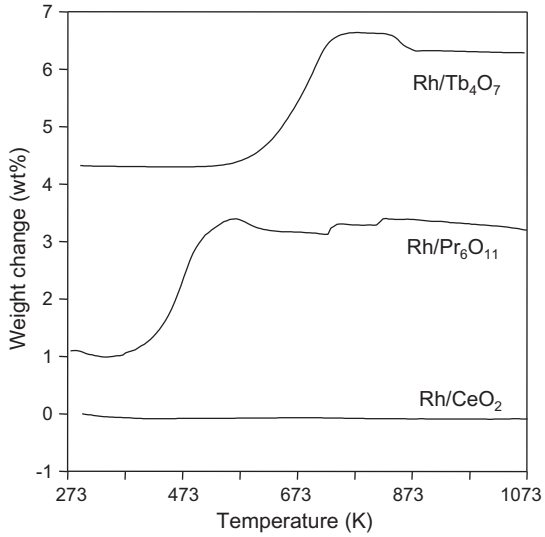

Fig. 9. TG profiles in an air flow for supported Rh catalysts used for XRD measurements (reduced at 873 K).

sults of the activity tests, we estimated the crucial value of x for triggering OR to be in the range $1.91 < (2-x) < 2.0$.

3.3. Catalyst support properties required for catalytic OR

The experimental results we have presented so far demonstrate that although CeO_2, Pr_6O_{11}, and Tb_4O_7 all have redox properties, those of CeO_2 are different from those of Pr_6O_{11} and Tb_4O_7. In this section, we will discuss the redox properties of the supports required for triggering OR at room temperature, starting with the catalyst reduction process. O_2 absorption measurements revealed that CeO_2 in Rh/CeO_2 was reduced to $CeO_{1.91}$ at 873 K. In contrast, XRD measurements indicated that Pr_6O_{11} in Rh/Pr_6O_{11} and Tb_4O_7 in Rh/Tb_4O_7 were reduced to Pr_2O_3 and Tb_2O_3, respectively, even at 473 K. During the oxidation process, reduced CeO_2 was oxidized completely and rapidly at room temperature with strong heat evolution, whereas a temperature above 373 or 573 K was required to oxidize Pr_2O_3 and Tb_2O_3, as indicated by TG measurements.

Note that both Pr_6O_{11} and Tb_4O_7 could be reduced and oxidized at temperatures higher than 373 and 573 K, respectively, that is, these materials exhibited OSC at moderate temperatures. However, if a catalyst support is to be useful for the new catalytic OR process, it should undergo reduction by H_2 and the reduced oxide should undergo oxidation at room temperature. Therefore, CeO_2 was the only suitable support among those tested in this study. We suggest that the excellent stability of the quadrivalent state of Ce (CeO_2) and the strong redox properties of the CeO_2/CeO_{2-x} couple [41] played important roles in the suitability of this support. In addition, our results indicate that the design considerations for supports for the new catalytic OR process are completely different from the considerations for OSC materials for conventional use.

3.4. Role of Rh and CeO_2 in cycle tests

To determine the roles of Rh and CeO_2 in the cycle tests, we ran the new catalytic OR process described in Fig. 1 with Rh/CeO_2 and bare CeO_2. Prior to the first cycle, the catalysts were reduced in H_2 at 873 K, and feed gas for OR of n-C_4H_{10} was supplied to the catalyst at room temperature (Fig. 10). For both catalysts, complete conversion of O_2 and 90% conversion of n-C_4H_{10} were obtained. However, the product yields for the two catalysts were completely different. As already mentioned in Section 3.1, OR over Rh/CeO_2

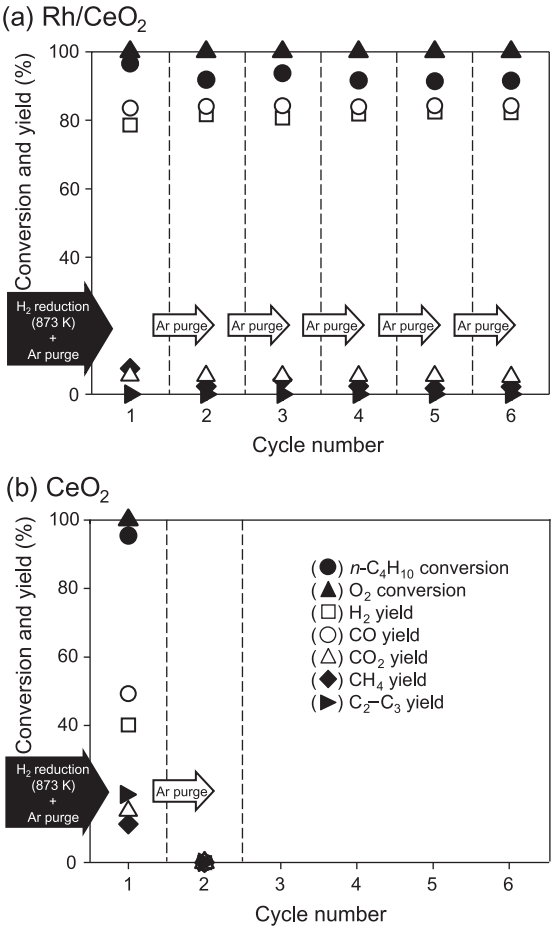

Fig. 10. Catalytic activity of (a) Rh/CeO_2 and (b) CeO_2 reduced at 873 K in OR cycle tests.

afforded high H_2 and CO yields and low CO_2 and CH_4 yields, which indicates that n-C_4H_{10} reforming and a small amount of methanation of CO and CO_2 occurred. In contrast, when the OR process was carried out over bare CeO_2, CO, CO_2, CH_4, and C_2–C_3, hydrocarbons were obtained in yields of 52%, 15%, 11%, and 20%, respectively. These results indicate that combustion and cracking of n-C_4H_{10} were the main reactions triggered over bare CeO_2. The results confirm that the heat produced by CeO_{2-x} to CeO_2 was essential for triggering n-C_4H_{10} combustion, and that the role of the supported Rh was to catalyze n-C_4H_{10} reforming.

Thirty-five minutes after the start of the first cycle, the reaction was terminated by the substitution of the feed gas with Ar, and the catalyst was cooled to room temperature. This feed–purge sequence was repeated five more times. The same products were produced during all the cycles after the reactant was fed to the Rh/CeO_2 catalyst. Complete conversion of O_2 and 90% conversion of n-C_4H_{10} were achieved for all the experiments. After the second cycle, Rh/CeO_2 was clearly reduced *in situ* during the OR (see Fig. 1). At the steady states, O_2 in the reaction mixture was consumed by combustion at the inlet of the catalyst bed, and H_2 that was produced reduced the catalyst at the rest of the catalyst bed. A catalyst bed temperature of 1133 K (Fig. 2) must have been sufficiently high to reduce the CeO_2 in Rh/CeO_2. A slight decrease in n-C_4H_{10} conversion as the number of cycles increased implies that slight sintering of the catalyst occurred. With the decrease in n-C_4H_{10} conversion, the decrease in CH_4 yield was observable. These results indicate that CH_4 was produced by methanation of CO and CO_2. In case of OR, exothermic combustion and endothermic reforming proceed at inlet and exit of catalyst layer, respectively.

We can assume that temperature of exit of the catalyst bed is rather low and methanation occurs.

Note that no reactions were observed over bare CeO_2 upon exposure to the feed gas after Ar purge following the first cycle. Because the H_2 concentrations in the product gas were rather low, we speculate that reduction of CeO_2 was not sufficient to trigger reactions at room temperature. Our results demonstrate that Rh was essential for the new catalytic OR process because it catalyzed the reforming reaction to produce H_2 at a concentration high enough for *in situ* reduction of CeO_2 to CeO_{2-x}.

4. Conclusions

We investigated the effects of the nature of the catalyst support on a new catalytic OR procedure (Fig. 1) that can be expected to permit the development of self-sufficient reforming systems that will be required for a new generation of fuel-cell applications. Oxidative reforming of n-C_4H_{10} was triggered rapidly and repeatedly at room temperature by the heat produced by the spontaneous oxidation of a reduced form (CeO_{2-x}) of the catalyst support. CeO_2 was reduced *in situ* to CeO_{2-x} by H_2 formed during the oxidative reforming. Unlike Pr_6O_{11} and Tb_4O_7, CeO_2 had unique redox properties: it was reduced to $CeO_{1.91}$ by treatment with H_2 at 873 K and was oxidized to CeO_2 at room temperature. These unique properties were crucial for triggering oxidative reforming of n-C_4H_{10} at room temperature. Our results suggest that the design requirements for supports for the new catalytic OR process are completely different from those of supports for OSC materials used in conventional catalytic processes, where redox capacity at moderate temperature (not as low as room temperature) is needed, such as catalytic oxidation and the automotive three-way reaction. In addition, Rh was essential because it catalyzed the reforming reaction and produced H_2 at the high concentration required for *in situ* reduction of CeO_2 to CeO_{2-x}.

Acknowledgments

K. Sato was supported by JSPS Research Fellowships for Young Scientists. This work was partly supported by KAKENHI (08J11493), a Grant for Researches from The Japan Petroleum Institute, the Nippon Sheet Glass Foundation for Materials Science and Engineering and the Linking mechanism of research results to practical applications from the Japan Science and Technology Agency.

References

[1] V. Dusastre, Nature 414 (2001) 331.
[2] F. Bruijn, Green Chem. 7 (2005) 132–150.
[3] R.L. Borup, M.A. Inbody, T.A. Semelsberger, J.I. Tafoya, D.R. Guidry, Catal. Today 99 (2005) 263–270.
[4] P.K. Cheekatamarla, C.M. Finnerty, J. Power Sources 160 (2006) 490–499.
[5] B.C.H. Steele, A. Heinzel, Nature 414 (2001) 346–352.
[6] J.N. Wilson, R.A. Pedigo, F. Zaera, J. Am. Chem. Soc. 130 (2008) 15796–15797.
[7] M. Shiraga, D. Li, I. Atake, T. Shishido, Y. Oumi, T. Sano, K. Takehira, Appl. Catal. A: Gen. 318 (2007) 143–154.
[8] K.A. Williams, L.D. Schmidt, Appl. Catal. A: Gen. 299 (2006) 30–45.
[9] K. Faungnawakij, R. Kikuchi, N. Shimoda, T. Fukunaga, K. Eguchi, Angew. Chem. Int. Edit. 47 (2008) 9314–9317.
[10] M.C. Alvarez-Galvan, R.M. Navarro, F. Rosa, Y. Briceño, M.A. Ridao, J.L.G. Fierro, Fuel 87 (2008) 2502–2511.
[11] V. Fierro, O. Akdim, C. Mirodatos, Green Chem. 5 (2003) 20–24.
[12] S. Velu, K. Suzuki, T. Osaki, Chem. Commun. (1999) 2341–2342.
[13] M. Prettre, Ch. Eichner, M. Perrin, Trans, Faraday Soc. 42 (1946) 335b–339.
[14] D. Dissanayake, M.P. Rosynek, K.C.C. Kharas, J.H. Lunsford, J. Catal.132 (1991) 117–127.
[15] E. Ruckenstein, Y.H. Hu, Appl. Catal. A: Gen. 183 (1999) 85–92.
[16] T. Shishido, M. Sukenobu, H. Morioka, M. Kondo, Y. Wang, K. Takaki, K. Takehira, Appl. Catal. A: Gen. 223 (2002) 35–42.
[17] K. Nagaoka, K. Sato, S. Fukuda, S. Nakashiki, H. Nishiguchi, J.A. Lercher, Y. Takita, Chem. Mater. 20 (2008) 4176–4178.
[18] H. Jung, W.L. Yoon, H. Lee, J.S. Park, J.S. Shin, H. La, J.D. Lee, J. Power Sources 124 (2003) 76–80.
[19] C.A. Leclerc, J.M. Redenius, L.D. Schmidt, Catal. Lett. 79 (2002) 39–44.
[20] L.D. Schmidt, E.J. Klein, C.A. Leclerc, J.J. Krummenacher, K.N. West, Chem. Eng. Sci. 58 (2003) 1037–1041.
[21] M.Y. Sinev, V.Y. Bychkov, V.N. Korchak, O.V. Krylov, Catal. Today 6 (1990) 543–549.
[22] C. Serre, F. Grain, G. Belot, G. Maire, J. Catal. 141 (1993) 9–20.
[23] M.M. Mohamed, S.M.A. Katib, Appl. Catal. A: Gen. 287 (2005) 236–243.
[24] M. Luo, Z. Yan, L. Jin, J. Mol. Catal. A: Chem. 260 (2006) 157–162.
[25] M. Abecassis-Wolfovich, M.V. Landau, A. Brenner, M. Herskowitz, J. Catal. 247 (2007) 201–213.
[26] M. Adamowska, S. Muller, P.D. Costa, A. Krzton, P. Burg, Appl. Catal. B: Environ. 74 (2007) 278–289.
[27] X. Ma, H. Sun, Q. Sun, X. Feng, H. Guo, B. Fan, S. Zhao, X. He, L. Lv, Catal. Commun. 12 (2011) 426–430.
[28] E.C. Su, C.N. Montreuil, W.G. Rothschild, Appl. Catal. 17 (1985) 75–86.
[29] J.G. Numan, H.J. Robota, M.J. Cohn, S.A. Bradley, J. Catal. 133 (1992) 309–324.
[30] S.E. Golunski, H.A. Hatcher, R.R. Rajaram, T.J. Truex, Appl. Catal. B: Environ. 5 (1995) 367–376.
[31] S. Bernal, G. Blanco, M.A. Cauqui, M.P. Corchado, C. Larese, J.M. Pintado, J.M. Rodríguez-Izquierdo, Catal. Today 53 (1999) 607–612.
[32] J. Kašpar, P. Fornasiero, M. Graziani, Catal. Today 50 (1999) 285–298.
[33] G. Adachi, N. Imanaka, Chem. Rev. 98 (1998) 1479–1514.
[34] M.Y. Sineve, G.W. Graham, L.P. Haack, M. Shelef, J. Mater. Res. 11 (1996) 1960–1971.
[35] S. Bernal, G. Blanco, M.A. Cauqui, P. Corchado, J.M. Pintado, J.M. Rodríguez-Izquierdo, Chem. Commun. (1997) 1545–1546.
[36] C.K. Narula, L.P. Haack, W. Chun, H.-W. Jen, G.W. Graham, J. Phys. Chem. B 103 (1999) 3634–3639.
[37] Z. Song, W. Liu, H. Nishiguchi, A. Takami, K. Nagaoka, Y. Takita, Appl. Catal. A: Gen. 329 (2007) 86–92.
[38] T. Takeguchi, S. Manabe, R. Kikuchi, K. Eguchi, T. Kanazawa, S. Matsumoto, W. Ueda, Appl. Catal. A: Gen. 293 (2005) 91–96.
[39] D. Li, M. Shiraga, I. Atake, T. Shishido, Y. Oumi, T. Sano, K. Takehira, Appl. Cat. A: Gen. 321 (2007) 155–164.
[40] K. Sato, K. Nagaoka, H. Nishiguchi, Y. Takita, Int. J. Hydrogen Energy 34 (2009) 333–342.
[41] T. Sata, M. Yoshimura, J. Ceram. Assoc. Jpn. (Yogyo-Kyokai-Shi) 76 (1968) 116–122.